Journal of Geography and Cartography 2025, 8(1), 10320.
https://doi.org/10.24294/jgc10320

Article

Geoelectric, geomagnetic and vertical gradient investigation on Knossos area, Crete Island for detection of archaeological settlements

Panos Stephanopoulos*, Stavros Papamarinopoulos

Laboratory of Geophysics, Sector of Applied Geology & Geophysics, Department of Geology, School of Natural Sciences, University of Patras, 26504 Patras, Greece
*** Corresponding author:** Panos Stephanopoulos, stefanop@upatras.gr

CITATION

Stephanopoulos P, Papamarinopoulos S. Geoelectric, geomagnetic and vertical gradient investigation on Knossos area, Crete Island for detection of archaeological settlements. Journal of Geography and Cartography. 2025; 8(1): 10320. https://doi.org/10.24294/jgc10320

ARTICLE INFO

Received: 13 November 2024
Accepted: 24 December 2024
Available online: 9 January 2025

Abstract: A Detailed geophysical investigation was conducted on Knossos territory of Crete Island. Main scope was the detection of underground archaeological settlements. Geophysical prospecting applied by an experienced geophysical team. According to area dimensions in relation to geological and structural conditions, the team designed specific geophysical techniques, by adopted non-catastrophic methods. Three different types of geophysical techniques performed gradually. Geophysical investigation consisted of the application of geoelectric mapping and geomagnetic prospecting. Electric mapping focusses on recording soil resistance distribution. Geomagnetic survey was performed by using two different types of magnetometers. Firstly, recorded distribution of geomagnetic intensity and secondly alteration of vertical gradient. Measured stations laid along the south-north axis with intervals equal to one meter. Both magnetometers were adjusted on a quiet magnetic station. Values were stored in files readable by geophysical interpretation software in XYZ format. Oasis Montaj was adopted for interpretation of measured physical properties distribution. Interpretation results were illustrated as color scale maps. Further processing applied on magnetic measurements. Results are confirmed by overlaying results from three different techniques. Geoelectric mapping contributed to detection of a few archaeological targets. Most of them were recorded by geomagnetic technique. Total intensity aimed to report the existence of magnetized bodies. Vertical gradient detected subsurface targets with clearly geometrical characteristics.

Keywords: geophysical investigation; geomagnetic intensity; soil resistance; vertical gradient

1. Introduction

Knossos territory belongs in the subarea of Crete Island. Located in Central South Crete, specifically south of Heraklion town (**Figure 1**). In ancient times Knossos had been involved in the Minoan empire. It was acting as the main capital wherein located Minoan palace. During 1991 the University of Cambridge requested contribution in geophysical investigation on Knossos area. Request accepted by Lab of Geophysics, University of Patras and a specialized team begun journey for Crete Island. The geophysical team examined territory specifications and applied electric and magnetic non-destructive techniques [1–11]. Electric prospecting focuses on soil resistance distribution. As electrometer was chosen the Geoscan RM4. Main scope was alteration of soil resistance on specific depth by adopting twin-probe technique. Alternatively magnetic prospecting applied by two different types of magnetometers proton and fluxgate. Two of the same kind proton magnetometers are utilized for total intensity recording. One was acting as base by measuring drift values every ten seconds. The second unit record geomagnetic field value along the south-north axis. The vertical gradient of magnetic field is recorded by using fluxgate magnetometer such as

Geoscan FM36. Bothof magnetometers were adjusted on a magnetic quiet point. Also, fluxgate microcomputer was updated with geophysical grid dimensions. The survey was performed by measuring discreet points stations on profiles along the south-north axis. Discreet data stations and profiles were measured at one meter interval. By adopted Oasis Montaj executive geophysical software, distribution of measured physical properties was presented as color maps with represented color scale bar.

Figure 1. Map of Crete.

Geological and structural setting

Crete geology consisted of Neogene and Upper Miocene structures. Specifically, there were two geological formations named Finikia and Ag. Varvara. The first formation consisted of white homogenous marls, clays structure with gray color and brown thin-bedded intercalations. Base of formation consisted in general from unsorted agglomerate with influence by white homogeneous marls, limestones and marls, greenish clays and prenoegene rocks. Finikia formation overlays incompatible on Ag. Varvara formation.

The Second formation consisted mostly of bioclastic and reef limestones, which locally could be conglomerate or agglomerate. Laterally seemed to be passed into alternating foliated homogenous calcium marls or even limestones. Occasionally were found with local unconformity with underlying formation [12,13]. In **Figure 2** illustrated geological map of Crete, indicating Knossos area.

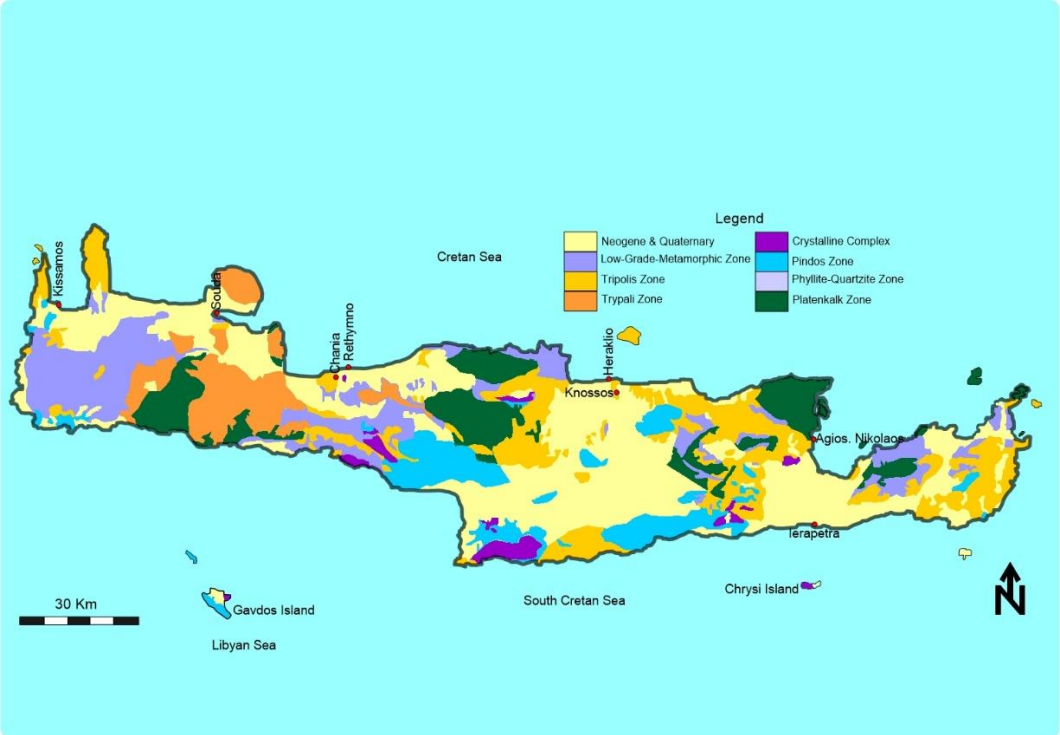

Figure 2. Geological map of Crete.

2. The used geophysical techniques and their limits

Knossos field topography characterized as level ground with very few points of discriminations. As main scope of the project was the detection of possible underground archaeological settlements in a depth equal to 1.5 to 2 meters. According to that, geophysical survey was adjusted and performed in a non-destructive way. As main techniques were chosen electric and magnetic prospecting in relation to existing geological formations. Survey field had been divorced in square geophysical grids with acme equal to 20 meters (**Figure 3**) [14–18]. Borders of grids were represented by adopting red wooden marks (no magnetic material). Each of them had been addressed by using unique name consisted by name of area, type of measurements, year. By adopting an electrometer as Geoscan RM4 (**Figure 4**), distribution of soil resistance recorded on specific depth along horizontal layer. During measurements two pairs of electrodes were involved. One of them was acting as base, while the other pair measured discreet points stations along the south-north axis with interval equal to one meter. Both electrode's pairs consisted of a potential and current electrode. The electrode pair distance was set equal to 0.75 meters. The unmovable pair was located away from mobile at a distance at least equal to fifteen times internal distance (pair distance). The above technique was known as twin-probe (**Figure 5**), ideal for mapping purposes [19,20], devoid by topographical alterations. Each measured point of soil resistance was stored on data logger or alternative on paper grid schedule. Before the main survey, location of electrodes was tested in case of artifact noise. By adopted shifted mode, electrodes were acting as mobile and base. Two different values of soil resistance were recorded. The difference between the two mentioned values should be equal to one ohm. In that case measurements accepted; alternatively highest difference values were rejected. In case of rejection another base point was examined

through the same procedure. The penetration depth of twin-probe arrangement was equal to three times the pair distance. Magnetic prospecting utilized by proton [21] and differential magnetometers. That technique corresponded to a very rapid method [8,22–25] which could be disturbed by susceptibility variations [3,10,26–28] from subsurface archaeological targets, according to sensor sensitivity. Two such kind of instruments (proton magnetometers) type Elsec 820 (**Figure 6**), were involved during geomagnetic investigation. One of them was located outside the main line of geophysical grids on a quiet magnetic point, acting as base station [29–32]. During magnetic survey, the base recorded drift intensity by interval of ten seconds. The second unit recorded magnetic intensity variations inside grids profiles along the south-north axis with one meter interval. Before the main survey procedure, proton magnetometers were adjusted to a quiet magnetic point [33,34]. The quiet magnetic point was checked by measuring discreet values of magnetic intensity by rotating proton magnetometer sensor with interval of 90 degrees. If the difference of values were less or equal than 1 nT, then that point was baptized as quite magnetic. Accordingly, the geophysical team was tested for artifact magnetic noise. Profiles on geophysical grids were utilized by using non-magnetic material, such as calibrated rope [29] per one meter. Two of them were laying at the south and north acme of geophysical grid, while third was perpendicular to previous. Both proton magnetometers were adjusted about internal time, value of magnetic field, memory erase [29,32]. Differential magnetometer (Geoscan FM36) (**Figure 7**) was adjusted on same quiet magnetic point along north, south, west, and east axis. Before the main survey procedure, fluxgate magnetometer was updated in relation to geophysical grids dimensions. Measurements were stored into instrument memory. After successful accomplish of field geophysical investigation, measurements were directed to pc through rs232 cable for further processing. Magnetic sources could be recorded up to a depth equal to three-five times the sensor height above surface ground [35].

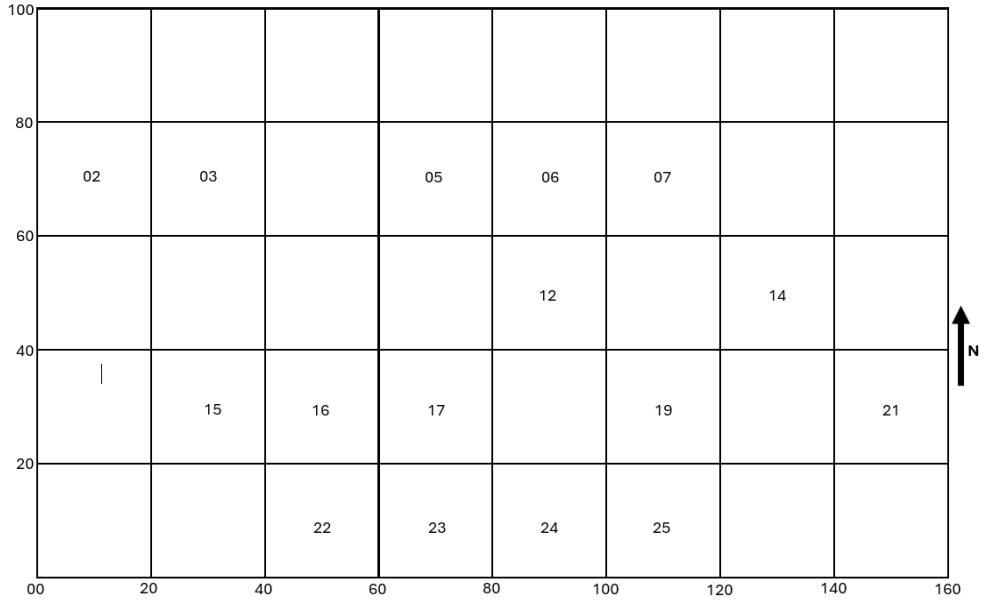

Figure 3. Location of geophysical grids.

Figure 4. Electrometer Geoscan RM4, with electrodes, base cable and frame.

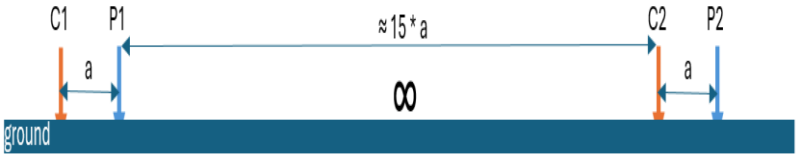

Figure 5. Twin-probe technique.

Figure 6. Proton magnetometer type Elsec 820.

Figure 7. Differential magnetometer Geoscan FM36.

3. Processing of measured values

Distribution of physical property was recorded by adopted specific instruments

along vertical or horizontal layer with no-destructive way, where real observation was unavailable. The survey focusses on differences between subsurface structures and surrounding environmental soil [9,16,26,27,36]. Electric mapping measurements were transferred to a pc through special software in relation to rs232 cable. Otherwise, values were typed on surfer worksheets with direction same as during their collection on field. Data were examined for the existence of possible bad points which could be represented as valleys or hills, matter which could easily produce shadow phenomenon. Next, data were dimensioned according to area length. Dimensions were produced through special software [35] or alternatively by using specific surfer subroutines. Values were stored into specific file with unique code name and readable format (XYZ) by interpreted geophysical software.

Magnetic data transferred into pc files through specific software, through rs232 cable. Data from base station (proton magnetometer) and mobile magnetometer stored into specific ascii format file. Geomagnetic data were corrected from daily geomagnetic drift by subtracting mobile values file from responsive base file according recording time [18,36,37]. Before correction procedure, base station measurements were examined comprehensively in case of existing noisy points. In that case noise data were removed or substituted by average of previous and next values. In corrected measurements, basic value of geomagnetic intensity is added. Fluxgate measurements were processed by using the same way as total intensity without drift correction procedure. Accomplishing transfer, values were modified in readable XYZ format file by using specific software. Vertical gradient could provide horizontal position and shape information of subsurface targets [38]. Recorded measurements from three techniques combined by using statistical analysis and reduced to a level by calculating common average value [18].

Final data from both geophysical surveys were fed in specific database of Oasis Montaj software [26,31,32,39] for further interpretation. As result color maps illustrated distribution of physical properties such soil resistance, geomagnetic intensity, and vertical gradient. During color map development measurements interpolated by adopted Akima equation [40] with interval equal to ¼ of initial step during field procedure.

Advanced geophysical interpretation applied on magnetic measurements (Total & Differential). First, performed calculation of Z derivative on total intensity measurements [26,32,39,41]. Secondly, total intensity values redacted to North Magnetic Pole and Equator [7,32,39]. Noisy values were eliminated by performing downward and upward continuation [32]. Amount of apparent magnetic susceptibility calculated on specific depths [26]. As last procedure enforcement three-dimensional Euler Deconvolution [26,42,43]. More details about advanced geophysical interpretation will be reported in the discussion paragraph.

4. Obtained results

Geoelectric mapping with twin-probe array divided the field area into subdomains consisting of low and high interesting structures. Some of them were illustrated with hot colors (orange until red), which represented structures as bad current conductors. These were presented with partially clear geometric characteristics.

Low soil resistance values indices structures existence in greater depth according to prospect of twin-probe array. Reduction of grids to mean average value through statistical analysis in relation with level coordinates, had as result the combination of measured geophysical grids. Geomagnetic technique seemed to be more effective in alterations of measured total intensity alterations along to a horizontal layer. That procedure applied with interval equal to one meter along the south-north axis. After necessity corrections, processing with oasis montaj software located enough geophysical anomalies, which covered most lengthening of total intensity map. Values represented by cold and hot colors. Cold values were indicated sources with low magnetic susceptibility or alternatively sources in greater depth, according to sensor sensitivity. Hot values represented the existence of magnetic source with high susceptibility contrast between structure and surrounding soil [44]. Total intensity distribution reported clear geometric characteristics. Fluxgate application confirmed the existence of magnetic sources with geometric characteristics. Application of mathematical filter on magnetic values through oasis montaj software, reported details which were not founded on normal total intensity map.

5. Discussion of results

Geomagnetic intensity distributed with floating values between 45,108 to 45,799 nT (**Figure 8**). The total intensity map is covered almost by the existence of measurements with clear geometric characteristics in most cases. Indication of lower values (cold colors) represented sources in greater depths or material of low magnetic response. For detailed results total intensity measurements interpreted through special mathematical algorithm for calculation of Z derivative [40] which could easily enhance the shallowest magnetic sources from collected data (**Figure 8**). The calculated Z gradient seemed to be divorced in smaller geophysical anomalies. After derivative procedure there was growth of magnetic dipoles and well-defined geometric characteristics (**Figure 8**). Calculation of X and Y derivatives (**Figure 8**) didn't plus new details relative to existing magnetic anomalies. Reduction (north magnetic pole, Equator) reported alteration of magnetic dipoles, expansion of geophysical anomalies and confirmation of geophysical anomalies existence respectively (**Figure 8**). Reduction to the north magnetic pole and equator gave the opportunity for illustration of more detailed information. Implementation of shaded relief at total intensity and calculated vertical gradient reported new information in relation to initial map (geometrical characteristics). For eliminating noise total intensity measurements are interpreted by performing upward and downward continuation [40]. **Figure 9** presented results from upward continuation between zero (0) to fifty (50) meters. Upward processing consisted of a clean filter without any artifact result. It was used to remove or minimize effects of shallow sources and noise in geophysical grids, with unrecognized geometrical characteristics. Geophysical anomalies seemed to have expanded. According to color scale bar total intensity was floating between 45,374 to 45,443 nT.

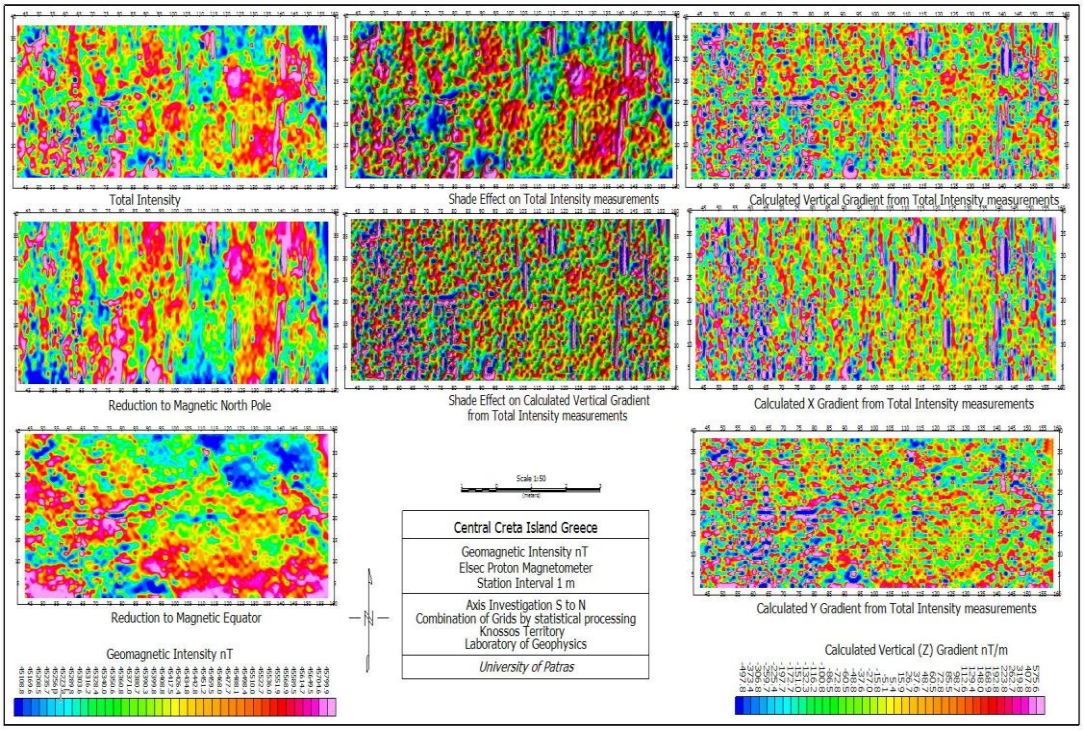

Figure 8. Distribution of total intensity & calculated vertical gradient (normal & shaded relief), reduction to north magnetic pole & equator, calculated verting gradient along X & Y axis.

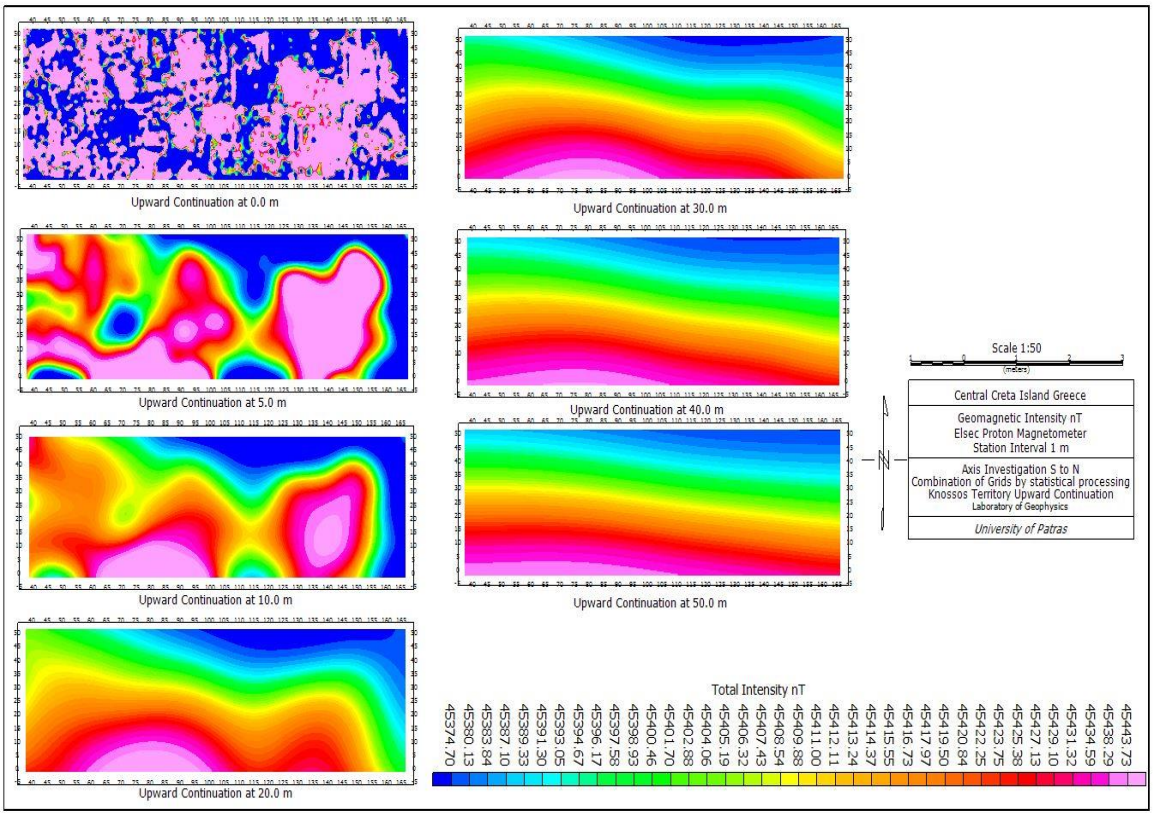

Figure 9. Application of upward continuation on total intensity measurements.

Existence of geometrical characteristics observed on downward continuation (**Figure 10**) after thirty meters depth. Such an application is used to enhance the responses from sources at depth by effectively bringing the plane of measurement

closer to the sources. According to the existing color scale bar, total intensity values were distributed between 4.04335e^{21} to 4.04339e^{21} nT. As next step of interpretation is calculation of apparent magnetic susceptibility by using floating depth values [40]. In **Figure 11** illustrated results from distribution of apparent susceptibility. Interpretation of measurements accomplished by combining total magnetic field, reduction to the magnetic pole, inclination, declination and susceptibility depth. A stronger apparent susceptibility was given at depth of 10 m (**Figure 11**). At two first depths (0,5) meters there were low apparent susceptibility targets. Highest values observed after ten meters depth and specific between 20- and 50-meters depth. Increasing apparent susceptibility indicating existence of possible magnetized structure. Euler deconvolution [40] algorithm performed as last total intensity data interpretation procedure (**Figure 12**). According to that equation, magnetic field is related with its gradient components to the location of the source of a geophysical anomaly. Homogeneity Degree expressed as "structural index". At each solution a prespecified square window in relation to the number of grid cells used during calculations. The window is in the center of each solution. Inversing distance from the center of window becomes one solution in Euler equation. Window dimensions are floating to include many solutions, but not large enough to include adjacent anomalies. The algorithm of Euler deconvolution applied gradually by using floating values of structural index between zero to three with interval equal to one. In **Figure 12** represented results in map schedule from that processing, which accomplished with small deviation error. Solutions presented by tighten cycles. Small diameters corresponded to low depth magnetic sources while, highest diameter represented deepest magnetic sources. By careful observation in **Figure 12** was obvious existence of distinct geometric characteristics at SI equal to 0, 1, 2 and 3. That matter ensured that existing magnetic underground targets corresponding to human remains, while geological evidence was absent.

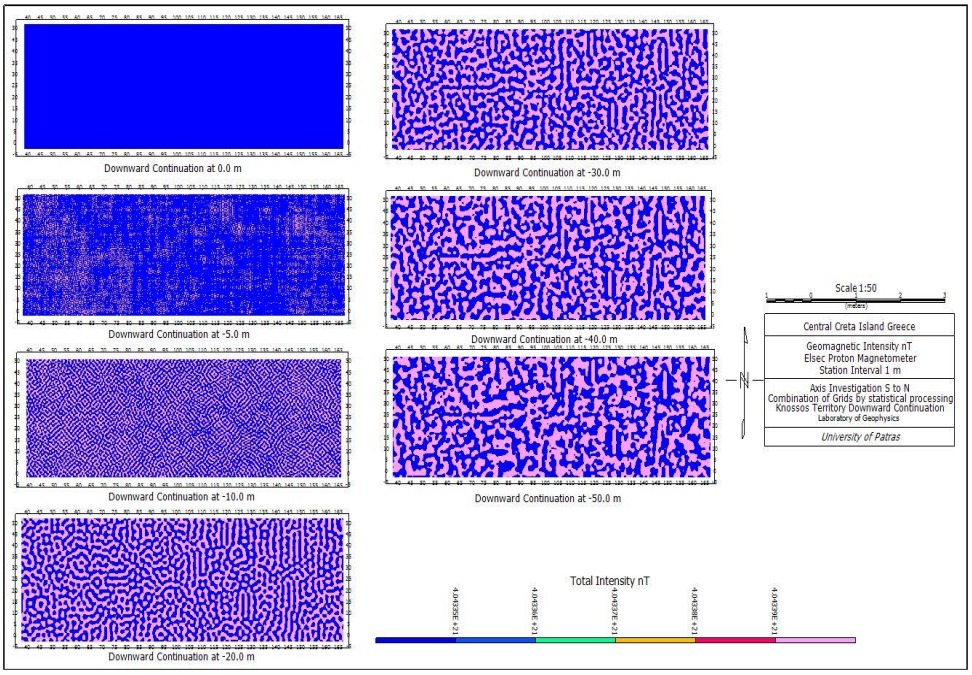

Figure 10. Appearance of downward continuation on total Intensity measurements.

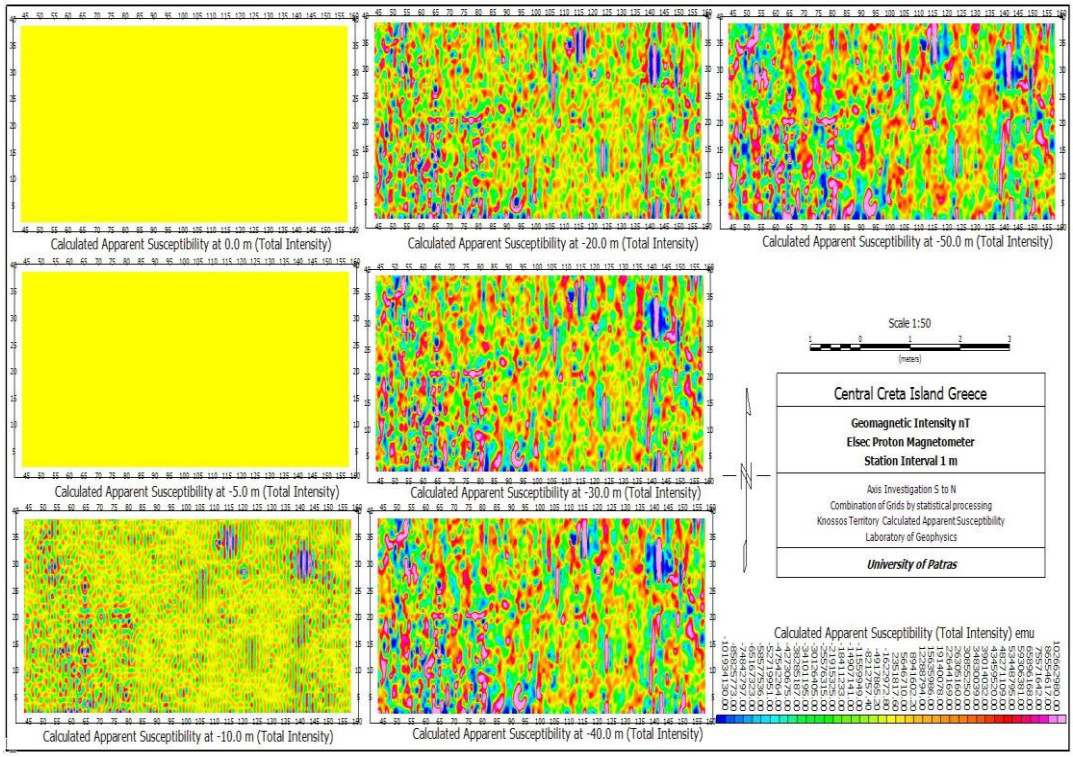

Figure 11. Distribution of apparent susceptibility on total intensity data.

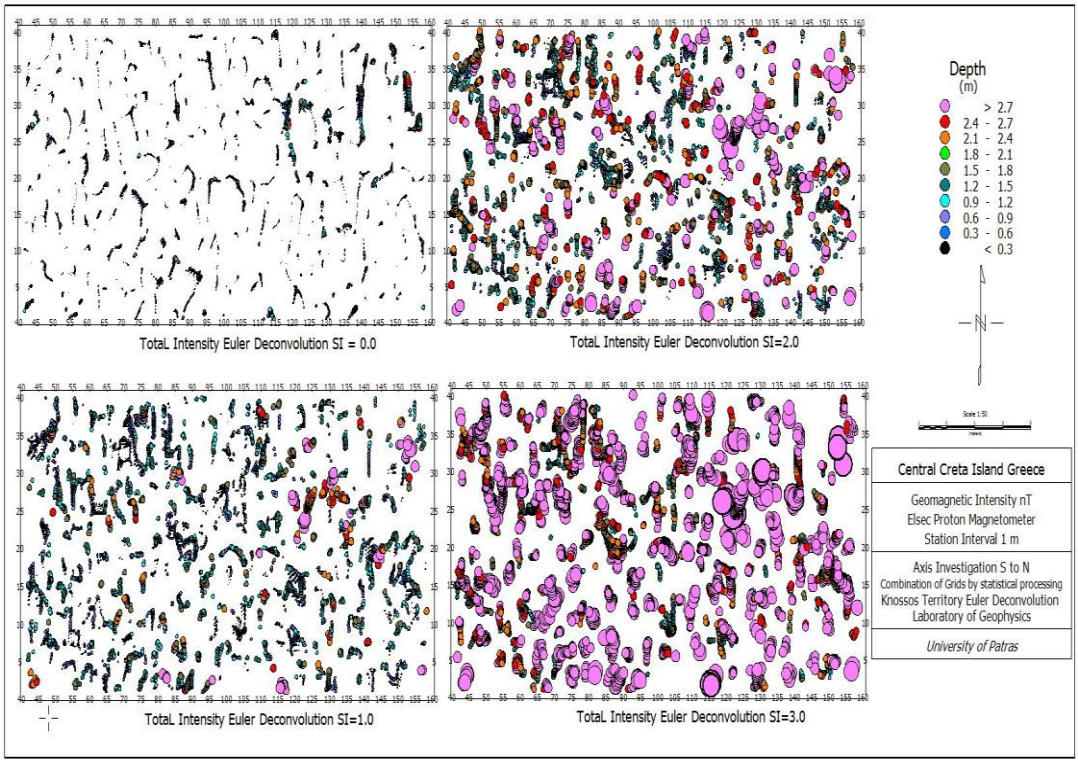

Figure 12. 3D Euler deconvolution on total intensity data.

Measured vertical gradient is illustrated in **Figure 13** with floating values between 44,987 to 45,012 nT/m. A huge number of magnetic dipoles located on vertical gradient allocation. Most of them are distributed on the west side of the map. In the center detected clearly geometrical characteristics which seemed like members

of an existing wall. That conclusion can be confirmed by shaded relief interpretation. By applied reduction to north magnetic pole (**Figure 13**) magnetic dipoles and geometric elements were detected more emphasized. Also, some magnetic dipoles were detected on the east side of that map, matter which was absent on initial presentation. Reduction to magnetic equator (**Figure 13**) just confirmed existence of magnetic dipoles on west side, with unrecognized geometrical elements. By applying the gradient calculation along X and Y axis, magnetic dipoles were reported on the east side of gradient map. (**Figure 13**). Existing geometrical characteristics were present with low clarity. Application of reduction to north magnetic pole and equator illustrated existence of many magnetic dipoles with low clarity. In **Figure 14** are presented results from upward continuation. Magnetic anomalies on vertical gradient were clearly detected at one meter continuation. Gradually expansion of vertical gradient was observed from fifth to fifty meters. That matter had as consequence the elimination of vertical gradient geophysical anomalies. Apparent susceptibility interpretation was given in **Figure 15** with floating values. That process performed gradually. Calculation of apparent susceptibility obtained at 5, 10, 20, 30, 40 and 50 m depth. The appearance of magnetic sources was present at 5 meters depth. After 5 meters depth the existence of that parameter increased gradually. Between 30 to 50 meters apparent susceptibility seemed to be with highest values. Between thirty-to-fifty-meter depth, geometrical elements were located like straight walls with evidence of corners. As last technique on vertical gradient data is applied Euler deconvolution (**Figure 16**). Main difference focuses on height value of magnetic sensor from ground surface. In the case of total intensity sensor height was equal to 0.3 m. In the case of vertical gradient, that parameter was increased to 0.5 m. In **Figure 16** presented results are presented from Euler deconvolution equation. Interpretation applied gradually with structural index from zero to three with one interval. Results from that procedure consisted of low deviation error. Magnetic sources were represented by cycles, with floating diameters (same as total processing). Cycles classification was characterized as tight. Observers could easily recognize existing geometrical elements after careful remark more than total intensity. The depth of magnetic sources is related to the increment of structural index value. In **Figure 17** reported soil resistance allocation. Geoelectric mapping technique performed on discreet geophysical grids, which were combined by using statistical analysis and reduction to specific level by using common average value. Soil resistance allocation illustrated by floating values between 27 to 48 ohms. High values extended in the greatest area of map. Alternatively low values located in specific subareas of given map in **Figure 17**. High level values corresponded to soil with low conductivity, represented material as bad current contactor. In opposite direction low values (cold color), corresponded to material with high conductivity, with other words good current contactor. Also, such indices could be mentioned existence of material in greater depth. Geometrical characteristics were clearly detected at most of the highest values of soil resistance. Application of shade relief confirmed the existence of geometrical characteristics, which seemed as linear geophysical anomalies. By applying analytic signal with Fast Fourier Transform soil resistance illustrated clear geometric structure at north side of soil resistance map. Also, at east side confirmed the existence of increased levels of that physical property. In **Figure 18** illustrated a specific interpretation of geophysical grids. By adopted special

subroutine of oasis montaj software, developed an overlay of three different maps. Measurements from each technique interpolated by using interval equal to ¼ of station and profile distance during field procedure. As next step firstly reported distribution of vertical gradient. On that overlayed alteration of total intensity and last soil resistance. By careful remark a researcher could easily recognize the existence of geometrical characteristics which indicated linear geophysical anomalies. Also, in the center of the overlayed map becomes clear existence of geophysical anomaly with square structure.

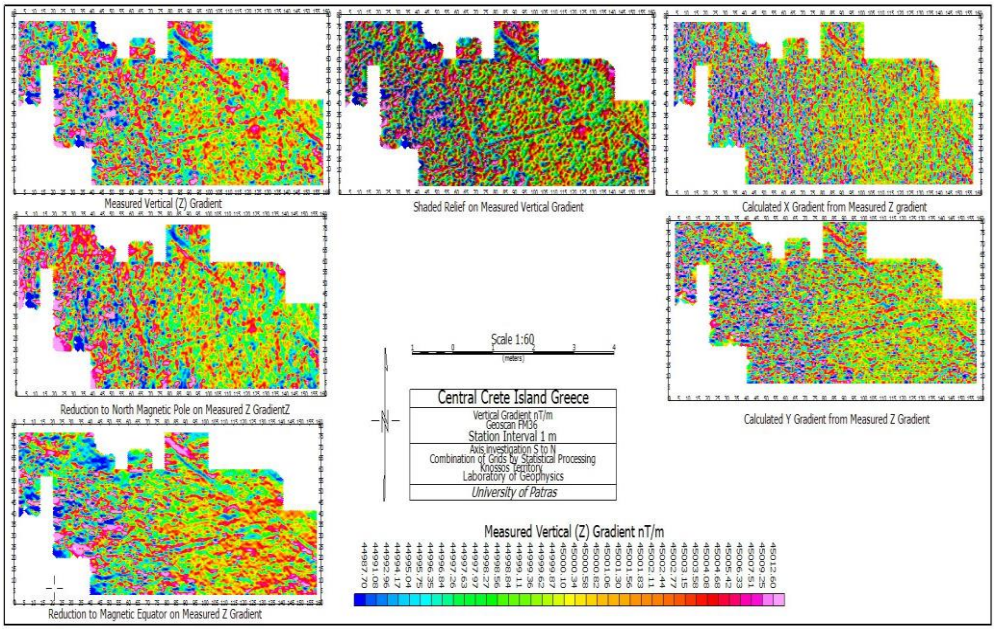

Figure 13. Distribution of measured vertical gradient (normal & shaded relief), reduction to north magnetic pole & equator, calculated verting gradient along X & Y axis.

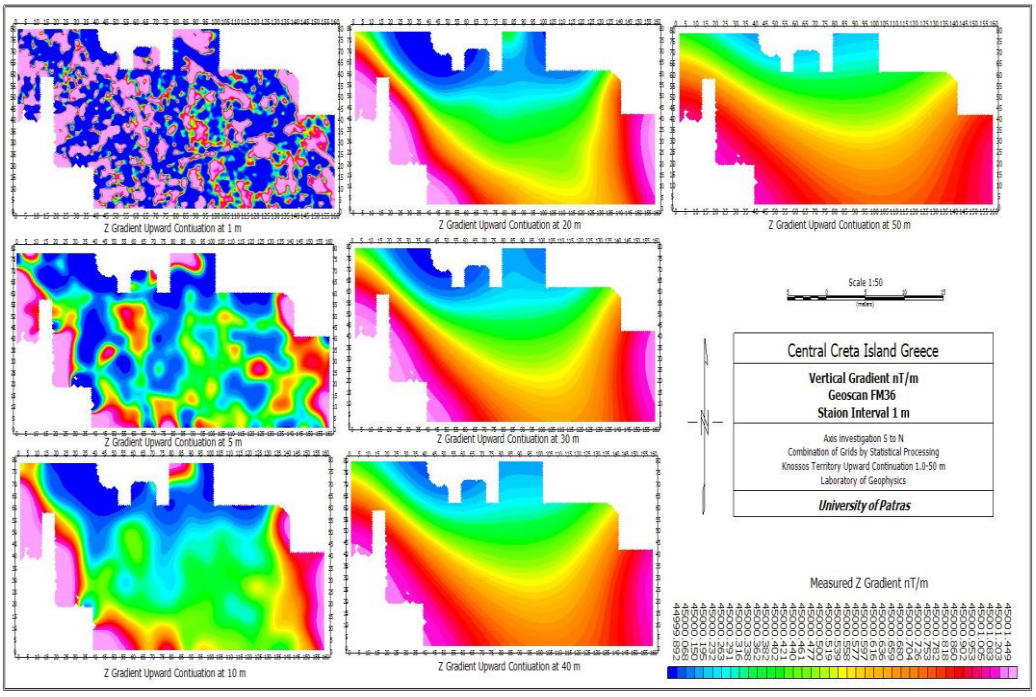

Figure 14. Application of upward continuation filter on measured vertical gradient data.

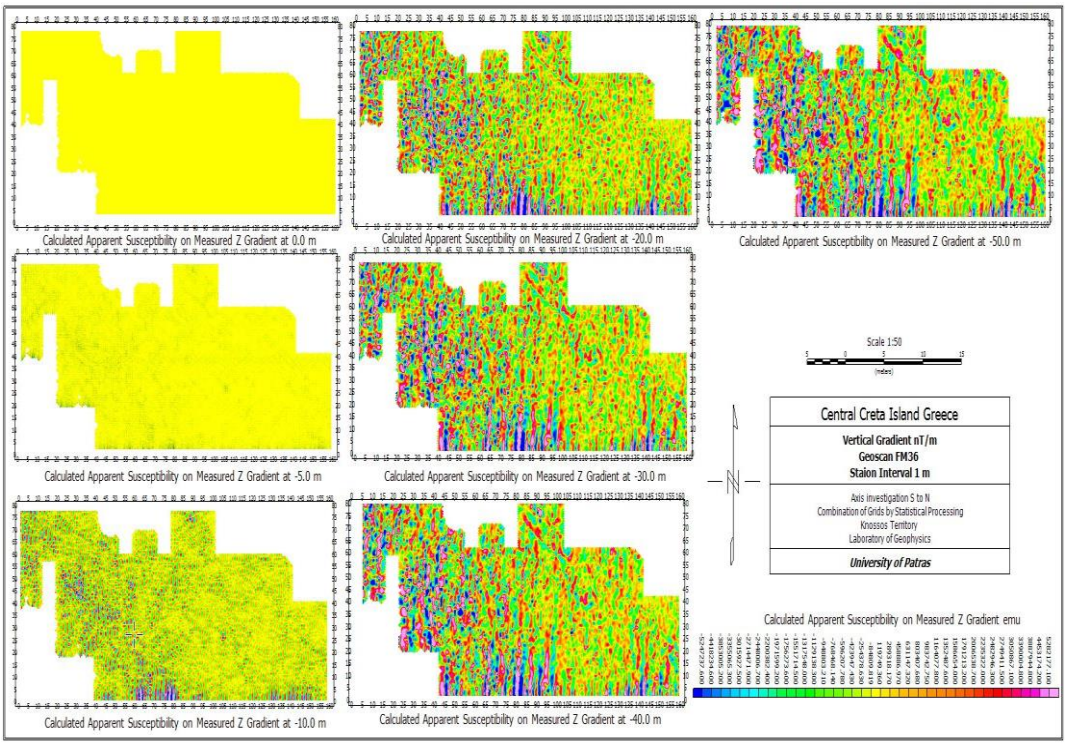

Figure 15. Distribution of apparent susceptibility on measured vertical gradient data.

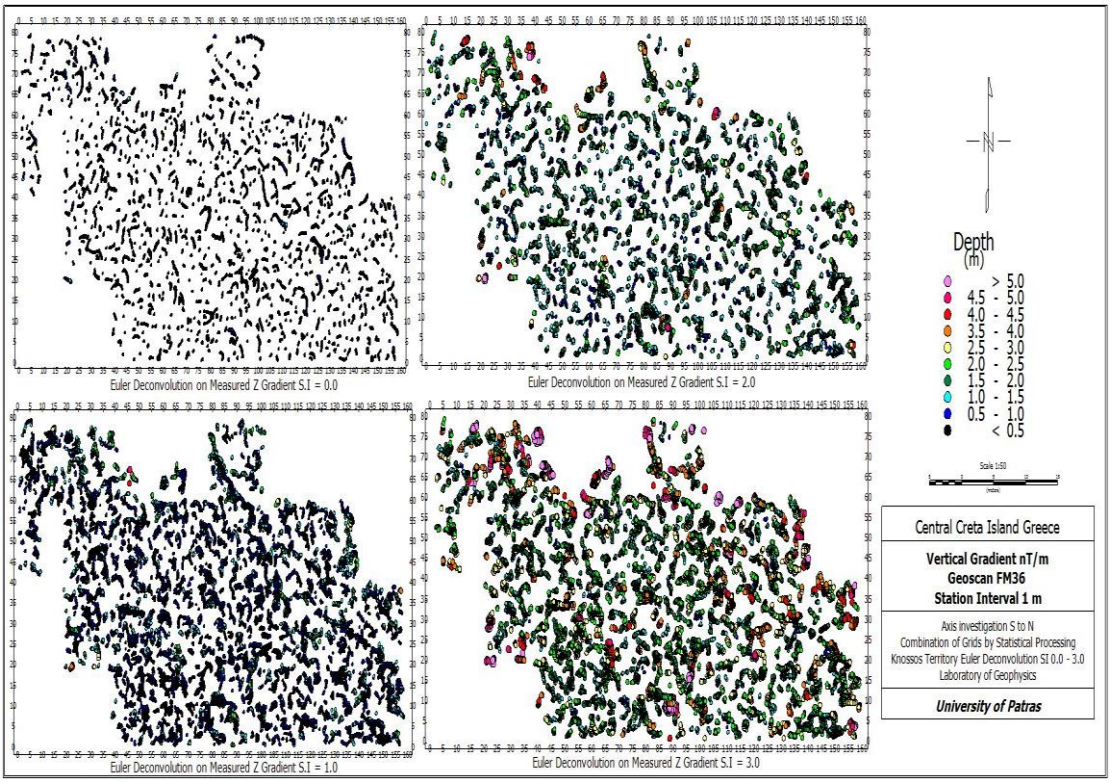

Figure 16. 3D Euler deconvolution on measured vertical gradient data.

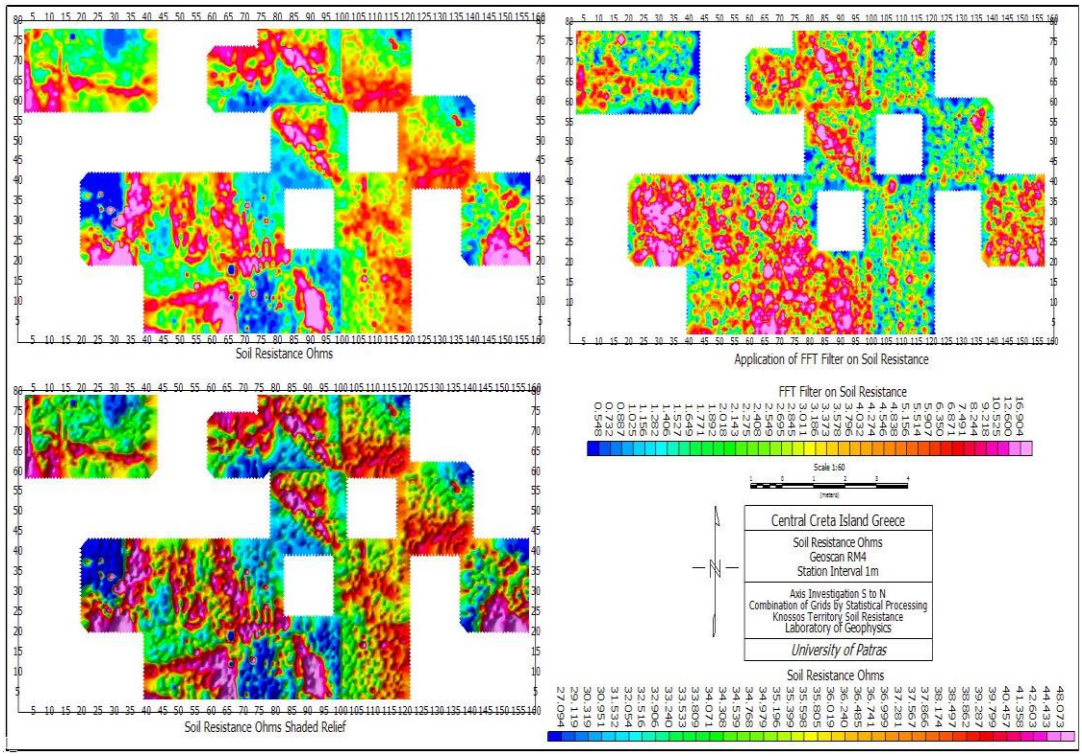

Figure 17. Soil resistance allocation on Knossos area (normal & shaded relief), application of FFT mathematical filter.

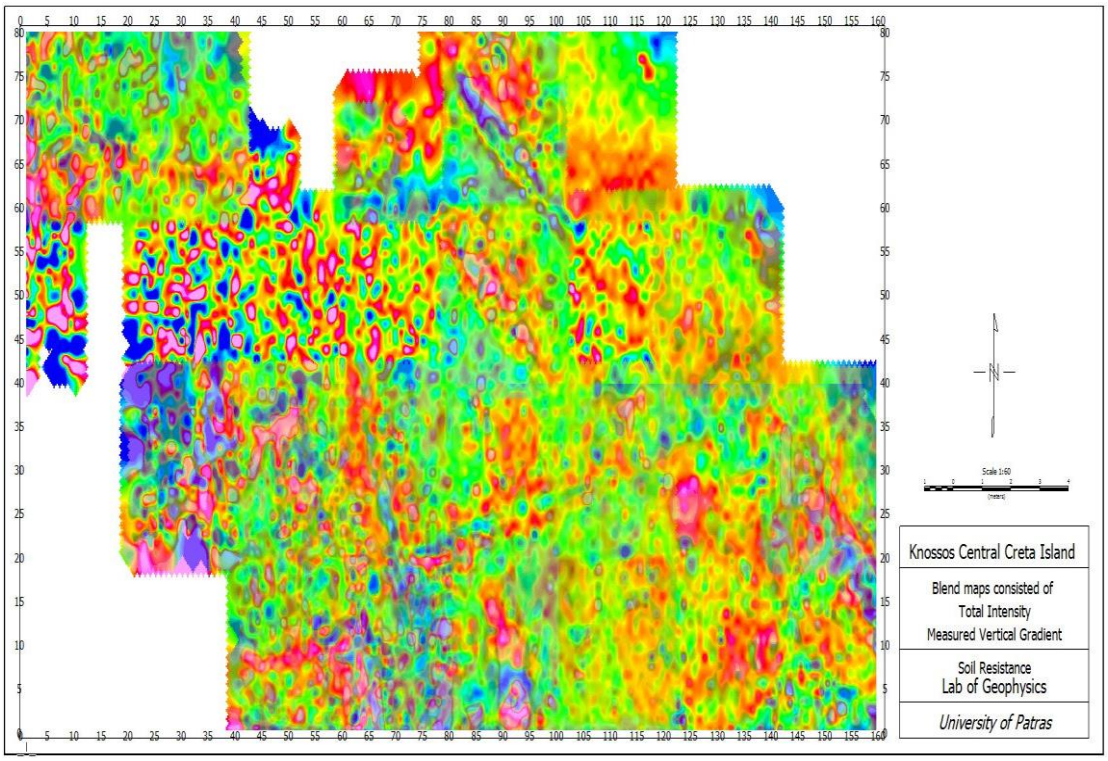

Figure 18. Blend map consisted of total intensity, measured vertical gradient and soil resistance.

6. Conclusion

Non-destructed geophysical techniques applied on Knossos territory for detection of archaeological settlements. Geophysical prospecting was performed by utilized two

different families of geophysical investigation. The survey area divided into several geophysical grids, focuses on recording of physical property distribution. Each of them had an acme equal to twenty meters. Combination of electric mapping with total intensity and vertical gradient applied gradually on each geophysical grid. Electric mapping recorded soil resistance allocation at depths of 1.5 to 2 m. The second technique focuses on total intensity recording until a depth 3 to five times the sensor height above ground surface. Third geophysical method applied vertical gradient, a technique with low noise [10,45]. The three above techniques were performed on separated data points along the south-north axis, located in parallel profiles with one meter interval. Measurements were interpreted through Oasis Montaj geophysical software. Recording of total intensity reported existence of magnetized structures. Some of them were reported to have hot colors meaning high susceptibility magnitude. In some areas of total intensity map there was evidence of low clarity geometrical characteristics. There was a great number of existing magnetic dipoles, which reported with combination of low and high values of total intensity. In the center of the total map there was evidence of linear geophysical anomalies. Application of shaded relief on total intensity measurements confirmed the existence of geometrical characteristics. Also, application of redaction to magnetic north pole and equator reported much more details of total intensity which were upsent on initial map. Upward and downward continuation cleared existing noise and illustrated existing evidence of human action at greater depths. Calculated apparent susceptibility certificate the existence of magnetic dipoles and confirmed in evidence of magnetized bodies. Euler deconvolution on total intensity values confirmed the existence of geometrical structures. Vertical gradient confirmed detection of geometrical characteristics from total intensity application. By using shaded relief filter on vertical gradient values, geometrical structures located better. The combination of reduction to north magnetic pole and equator just confirmed existence of human activity. Upward continuation illustrated high clarity linear geophysical anomalies at deeper levels. Calculation of apparent susceptibility on vertical gradient reported huge number of magnetic dipoles, which was detected by apparent susceptibility on total intensity values. Euler deconvolution on vertical gradient has as result the detection of geometrical structures, which was confirmed from total intensity Euler equation. Application of soil resistance divided area of survey in subareas of low and high interest. In some areas there was the existence of geometrical formations. That matter was confirmed by the application of shaded relief on soil resistance measurements. Also, by interpreted soil resistance values through analytical signal (Fast Fourier Transform), evidence of geometrical formations certificated. Overlay of maps from three different techniques confirmed the existence of geometrical characteristics which disentangle from existence of geological formation.

Author contributions: Conceptualization, PS and SP; methodology, PS and SP; software, PS; validation, PS and SP; formal analysis, PS; investigation, PS; resources, PS; data curation, PS; writing—original draft preparation, PS; writing—review and editing, PS and SP; visualization, PS; supervision, PS and SP; project administration, PS and SP; funding acquisition, SP. All authors have read and agreed to the published version of the manuscript.

Acknowledgments: The authors would like to thank Kollin Sell from University of Cambridge for absolute collaboration during geophysical prospecting on Knossos territory. Many thanks to the general secretary of research and development and NATO SfS program for equipment and total support. Also, many thanks to underground students from University of Patras for surveying supporting during field procedure.

Conflict of interest: The authors declare no conflict of interest.

References

1. Alashloo SYM, Saad R, Nawawi MNM, et al. Using Integrated Geophysical Techniques to Prospect an Unexcavated Archaeological Site at Sungai Batu, Kedah, Malaysia. Journal of Applied Sciences. 2011; 11(19): 3389-3396. doi: 10.3923/jas.2011.3389.3396
2. Arciniega-Ceballos A, Hernandez-Quintero E, Cabral-Cano E, et al. Shallow geophysical survey at the archaeological site of San Miguel Tocuila, Basin of Mexico. Journal of Archaeological Science. 2009; 36(6): 1199-1205. doi: 10.1016/j.jas.2009.01.025
3. Cardarelli E, Fischanger F, Piro S. Integrated geophysical survey to detect buried structures for archaeological prospecting. A case-history at Sabine Necropolis (Rome, Italy). Near Surface Geophysics. 2007; 6(1): 15-20. doi: 10.3997/1873-0604.2007027
4. Di Fiore B, Chianese D. Electric and magnetic tomographic approach for the geophysical investigation of an unexplored area in the archaeological site of Pompeii (Southern Italy). Journal of Archaeological Science. 2008; 35(1): 14-25. doi: 10.1016/j.jas.2007.02.020
5. Křivánek R. Application of geophysical methods for monitoring of surface and subsurface changes of origin archaeological terrains &ndahs; case studies of sites in the Czech Republic. The International Archives of the Photogrammetry, Remote Sensing and Spatial Information Sciences. 2015; XL-5/W7: 257-262. doi: 10.5194/isprsarchives-xl-5-w7-257-2015
6. Křivánek R, Tirpák J. Geophysical Survey and Changes in the Use of the Cultural Landscape. Interdisciplinaria Archaeologica Natural Sciences in Archaeology. 2023; XIV(1): 9-29. doi: 10.24916/iansa.2023.1.1
7. Martorana R, Capizzi P, Pisciotta A, et al. An Overview of Geophysical Techniques and Their Potential Suitability for Archaeological Studies. Heritage. 2023; 6(3): 2886-2927. doi: 10.3390/heritage6030154
8. Mateiciucová I, Milo P, Tencer T, et al. Geophysical survey at archaeological sites in northeastern Syria. ArchéoSciences. 2009; 33 (suppl.): 111-113. doi: 10.4000/archeosciences.1385
9. Milo P, Vágner M, Tencer T, et al. Application of Geophysical Methods in Archaeological Survey of Early Medieval Fortifications. Remote Sensing. 2022; 14(10): 2471. doi: 10.3390/rs14102471
10. Note N, Saey T, Gheyle W, et al. Evaluation of fluxgate magnetometry and electromagnetic induction surveys for subsurface characterization of archaeological features in World War 1 battlefields. Geoarchaeology. 2018; 34(2): 136-148. doi: 10.1002/gea.21700
11. Vagnon F, Comina C, Canepa MC, et al. Experiences and preliminary results of geophysical methods on historical statues. IOP Conference Series: Earth and Environmental Science. 2023; 1124(1): 012132. doi: 10.1088/1755-1315/1124/1/012132
12. Heraklion Sheet. Geological Map of Greece. Institute of Geology and Mineral Exploration, IGME; 1996.
13. Martha SO, Dörr W, Gerdes A, et al. The tectonometamorphic and magmatic evolution of the Uppermost Unit in central Crete (Melambes area): constraints on a Late Cretaceous magmatic arc in the Internal Hellenides (Greece). Gondwana Research. 2017; 48: 50-71. doi: 10.1016/j.gr.2017.04.004
14. Butler DK, Llopis JL, Briuer FL. Geophysical and Archaeological Investigations for Location of a Historic Cemetery, Fort Stewart, Georgia. Defense Technical Information Center; 1993. doi: 10.21236/ada267096
15. Papamarinopoulos P, Stefanopoulos P, Papaioannou M. Geopysical investigations in search of ancient Helike and the protection of the archaeological site versus the rapid building expansion. In: Proceedings of the international Symposium on Engineering Geology and the Environment Organized by the Greek National Group Of IAEG/Athens/Greece/23-27; June 1997.

16. Rizzo E, Dubbini R, Capozzoli L, et al. Preliminary geophysical investigation in the archaeological site of Bocca delle Menate (Comacchio, FE). Journal of Physics: Conference Series. 2022; 2204(1): 012107. doi: 10.1088/1742-6596/2204/1/012107
17. Saleh S, Saleh A, El Emam AE, et al. Detection of Archaeological Ruins Using Integrated Geophysical Surveys at the Pyramid of Senusret II, Lahun, Fayoum, Egypt. Pure and Applied Geophysics. 2022; 179(5): 1981-1993. doi: 10.1007/s00024-022-03010-2
18. Savvaidis A, Tsokas G, Tsourlos P, et al. A geophysical survey in the archaeological site of Archontiko, Yannitsa. Bulletin of the Geological Society of Greece. 2001; 34(4): 1379. doi: 10.12681/bgsg.17231
19. Branko M, Jana H, Dimc F. Comparison of different geophysical techniques in relation to archaeological data for settlement reconstruction - the case study of Nauportus. Slovenia; 2007.
20. Ogden J, Keay S, Earl G, et al. Geophysical Prospection at Portus: An Evaluation of an Integrated Approach to the Interpretation of Subsurface Archaeological Features, Computer Applications to Archaeology. Physical Sciences; 2009.
21. Jirků J, Belov T, Bárta J, et al. Geophysically – archaeological survey at the Hradčany square in Prague. EGRSE – Exploration Geophysics, Remote Sensing and Environment. 2018; (XXV/2): 20-26. doi: 10.26345/egrse-020-18-203
22. Bianco C, De Giorgi L, Giannotta MT, et al. The Messapic Site of Muro Leccese: New Results from Integrated Geophysical and Archaeological Surveys. Remote Sensing. 2019; 11(12): 1478. doi: 10.3390/rs11121478
23. Eppelbaum Lev. System of Potential Geophysical Field Application in Archaeological Prospection. In: Switzerland AG, D'Amico S, Venuti V (editors). Handbook of Cultural Heritage Analysis. Springer Nature; 2022.
24. Lowe KM, Fogel AS, Sneddon A. Archaeological geophysical survey of a Prehistoric Bronze Age site in Cyprus (Alambra Mouttes)—applications and limitations. Archaeological and Anthropological Sciences. 2017; 10(8): 1971-1989. doi: 10.1007/s12520-017-0508-3
25. Tonkov N. Complex magnetic and resistivity geophysical survey at the national archaeological reserve "Kabyle". Bulgarian Academy of Sciences; 2017
26. Abudeif AM, Abdel Aal GZ, Ramadan HS, et al. Geophysical Prospecting of the Coptic Monastery of Apa Moses Using GPR and Magnetic Techniques: A Case Study, Abydos, Sohag, Egypt. Sustainability. 2023; 15(14): 11119. doi: 10.3390/su151411119
27. Eppelbauir Lev V. Applicability of geophysical methods for localization of archaeological targets: An introduction. Geoinformatics. 2000; 11(1): 25-34. doi: 10.6010/geoinformatics1990.11.1_25
28. Grassi S, Morreale G, Lanteri R, et al. Integration of Geophysical Survey Data for the Identification of New Archaeological Remains in the Subsoil of the Akrai Greek Site (Sicily, Italy). Heritage. 2023; 6(2): 979-992. doi: 10.3390/heritage6020055
29. Bevan B. A Geophysical Survey at the West House, Richmond National Battlefield. Technical Report; 2002
30. Bevan B. Design of Geophysical Surveys. Technical Report; 2004.
31. Hannian S, Hijab B, Laftah A. Geophysical Investigation of Babylon archeological City, Iraq. Diyala Journal For Pure Science. 2021; 17(3): 1-24. doi: 10.24237/djps.17.03.533c
32. Olorunfemi MO, Ogunfolakan BA, Oni AG. Geophysical and Archaeological Survey in Igbo Oritaa (Iwo), Southwest Nigeria. African Archaeological Review. 2019; 36:535-552. doi: 10.1007/s10437-019-09357-7
33. Eppelbaum LV, Itkis SE, Khesin BE. Detailed magnetic survey unmasks prehistoric archaeological sites in israel. In: Proceedings of the 19th EEGS Symposium on the Application of Geophysics to Engineering and Environmental Problems; April 2006.
34. Scheiblecker M, Mühl S, Faßbinder J. Geophysical survey of single phase archaeological sites: New Global Perspectives on Archaeological Prospection. ResearchGate; 2019.
35. Panos S. Contribution of geophysics in solution of archaeological and environmental problems [PhD thesis]. University of Patras, Greece; 2002.
36. Rizzo E, Dubbini R, Clementi J, et al. Geomagnetic and FDEM Methods in the Roman Archaeological Site of Bocca Delle Menate (Comacchio, Italy). Heritage. 2023; 6(2): 1698-1712. doi: 10.3390/heritage6020090
37. Bárta J, Belov T, Frolík J, et al. Applications of Geophysical Surveys for Archaeological Studies in Urban and Rural Areas in Czech Republic and Armenia. Geosciences. 2020; 10(9): 356. doi: 10.3390/geosciences10090356
38. Shi Z, Tian G, Hobbs RW, et al. Magnetic gradient and ground penetrating radar prospecting of buried earthen archaeological remains at the Qocho City site in Turpan, China. Near Surface Geophysics. 2015; 13(5): 477-485. doi: 10.3997/1873-0604.2015033

39. Augie AI, Salako KA, Rafiu AA, et al. Geophysical Magnetic Data Analyses of the Geological Structures with Mineralization Potentials Over the Southern Part of Kebbi, NW Nigeria. Mining Science. 2022; 29. doi: 10.37190/msc222911
40. Oasis Montaj. Mapping and processing system. Oasis Montaj; 2008.
41. Filzwieser R, Olesen LH, Neubauer W, et al. Large-scale geophysical archaeological prospection pilot study at Viking Age and medieval sites in west Jutland, Denmark. Archaeological Prospection. 2017; 24(4): 373-393. doi: 10.1002/arp.1576
42. Papamarinopoulos StP, Papaioannou MG, Stefanopoulos P, et al. The Geophysical Discovery of a Second World War Battlefield in Central Crete During Construction Activities by a Building Company. Environmental & Engineering Geophysical Society; 1995.
43. Ahmed SB, El Qassas RAY, El Salam HFA. Mapping the possible buried archaeological targets using magnetic and ground penetrating radar data, Fayoum, Egypt. The Egyptian Journal of Remote Sensing and Space Science. 2020; 23(3): 321-332. doi: 10.1016/j.ejrs.2019.07.005
44. Lichtenberger A, Meyer C, Schreiber T, et al. Magnetic Prospection in the Eastern Lower City of Artashat-Artaxata in the Ararat Plain of Armenia. Electrum. 2022; 29: 109-125. doi: 10.4467/20800909el.22.008.15778
45. Fedi M, Florio G, Garofalo B, et al. Integrated geophysical survey to recognize ancient Picentias buried walls, in the Archaeological Park of Pontecagnano Faiano (Southern Italy). Annals of Geophysics. 2009; 51(5-6). doi: 10.4401/ag-3017